IMAGE PROCESSING TECHNIQUES APPLIED FOR PITTING CORROSION ANALYSIS

Tawfeeq A. Alkanhal[1]

[1]*Research Center director of Engineering and Applied Science, Faculty of Engineering, Majmaah University, Saudi Arabia,*

Abstract

In order to study the behavior of the early stage of pitting corrosion, an image analysis based on discrete wavelet packet transform and fractals was used. Image feature parameters were extracted and analyzed to characterize the pitting corrosion development with test time. It was found that the feature parameters: Shannon entropy, energy, fractal dimension and intercept increased with the test time. Therefore the image processing techniques were promising and effective tools to analyze and detect the pitting corrosion.

Keywords: *corrosion, pitting corrosion, surface topography, surface analysis, carbon steel, tap water*

----------***----------

1. INRRODUCTION

Pitting corrosion is localized accelerated dissolution of metals that occurs as a result of a breakdown of the otherwise protective passive film on the metal surface [1]. Pitting is regarded as one of the most dangerous and an insidious form of corrosion, since it often leads to perforation and to a consequent premature corrosion failure [2-5]. For general corrosion, the corrosion monitoring and the life prediction of the metal materials can be carried out without difficulty. However for the localized corrosion, the precise monitoring is difficult to manage reliably. Therefore, recent research efforts concentrate on the development of numerical descriptors and image processing techniques to monitor the localized corrosion.

Image analysis technique, which nowadays has become a worthwhile tool for being able to perform analyzes of fast, inexpensive and non-destructive for many processes. Image analysis is an appropriate tool to characterize qualitatively and quantitatively the early stage of the mechanism of damage by corrosion [6-9]. Pitting corrosion through pit numbers determination and its morphology characteristics was evaluated using image analysis [10-13]. The use of image analysis of corroded surfaces to determine the morphology and extent of pitting corrosion has not received much attention.

The objective of the present work is to use fractal and wavelet analysis to assess the growth of pitting corrosion with the test time for low carbon alloy steel.

2. IMAGE ANALYSIS TECHNIQUES

Various methods exist for characterization of surface topography and extract the relevant features. Wavelet transforms and fractals were adopted in this study, since, unlike other methods, they characterize surface topographical features over different scales. They are described briefly below.

2.1 Wavelet Packet Decomposition

The main advantage of using wavelets is that it provides multi-resolution analysis. Multi-resolution processing can improve the image quality obtained from microscopy techniques, such as SEM and others. Wavelet decomposition and its extension, wavelet packet decomposition, have gained popular applications in the field of signal/image processing and classification because of many outstanding properties of wavelet packet. Wavelet transforms enable the decomposition of the image into different frequency subbands, similar to the way the human visual system operates [14].

In 2-D discrete wavelet packet transforms (2-D DWPT); an image is split into one approximation and three detail images. The approximation are then split into a second-level approximation and detail images, and the process is recursively repeated. The standard 2-D DWPT can be described by a pair of filters; a low-pass filter h and a high-pass filter g [15]. The 2D discrete wavelet packet decomposition of an M x N discrete image x up to level p+1 $(0 \le P \le \min(\log_2 N + \log_2 M))$ is recursively defined in terms of the coefficients at level p as follows[14]:

$$c^{P+1}_{4K,(i,j)} = \sum_m \sum_n h(m)\, h(n)\, c^{P}_{K,(m+2i,n+2j)} \quad (1)$$

$$c^{P+1}_{4K+1,(i,j)} = \sum_m \sum_n h(m)\, g(n)\, c^{P}_{K,(m+2i,n+2j)} \quad (2)$$

$$c_{4K+2,(i,j)}^{P+1} = \sum_m \sum_n g(m)\, h(n)\, c_{K,(m+2i,n+2j)}^{P} \quad (3)$$

$$c_{4K+3,(i,j)}^{P+1} = \sum_m \sum_n g(m)\, g(n)\, c_{K,(m+2i,n+2j)}^{P} \quad (4)$$

Where C_0^0 is image x and K is an index of the nodes in the wavelet packet tree denoting each subband; h and g are the filter coefficients of low-pass and high-pass filters, respectively. Supposing that Haar basis has been used, h={-0:7071; 0:7071}, and g = {0:7071; 0:7071}. At each step, the image c_K^P is decomposed into four quarter-size images $c_{4K}^{P+1}, c_{4K+1}^{P+1}, c_{4K+2}^{P+1}, c_{4K+3}^{P+1}$. The capital letters (N or M) are maximum constants defined by the image size. However, small letters (m or n) are defined at each step. For example, when P = 5, P can be 1, 2, 3, or 4 and so on.

The Shannon entropy and the energy in different sub-bands are computed from the sub-band coefficient matrix as:

$$Entropy_P(k) = -\sum_i \sum_j \left|c_{k,(i,j)}^P\right|^2 \log \left|c_{k,(i,j)}^P\right|^2 \quad (5)$$

$$Energy_P(k) = -\sum_i \sum_j \left|c_{k,(i,j)}^P\right|^2 \quad (6)$$

Where Energy p(k) and Entropy p(k) are the energy and entropy of the image projected onto the subspace at node (p, k). The entropy of each sub-band provides a measure of the image characteristics in that sub-band. The energy distribution has important discriminatory properties for images and as such can be used as a feature for texture classification. From the equations above, it follows that the wavelet entropy is minimum when the image represents an ordered activity characterized by a narrow frequency distribution, whereas the entropy is high when an image contains a broad spectrum of frequency distribution.

2.2. Fractal Analysis

Fractal geometry is a well-known non-traditional method which has found many applications in science and engineering. It is common knowledge that many objects in nature are of irregular form which cannot be described by Euclidean geometry. These non-Euclidean objects are called fractals, and can be described by non-integer numbers. These non-integer numbers define the fractal dimension (FD) of an object. The main concept of fractal geometry analysis is that a fractal dimension can be considered as a quantitative measure of object surface heterogeneity because of its inherent self-similarity features. In a simplified representation, one could interpret the fractal dimension as a measure of heterogeneity of a set of points on a plane, or in space. FD can numerically characterize the variation in surface structure caused by corrosion [11], which corresponds to morphology changes in grey value images captured by microscopy techniques such as SEM or AFM.

A number of methods have been used to calculate fractal features of the surfaces such as Fourier, Kolmogorov, Korcak, Minkowski, root mean square, Slit Island, etc. These techniques differ in computational efficiency, numerical precision and estimation boundary. The most efficient procedure for measurement of the FD of surfaces, and one which allows characterization of anisotropic surface as well, seems to be through Fourier analysis [e.g. 16, 17]. Therefore, Fourier analysis is adopted to estimate fractal values in this work. For a surface image represented by the function I(x, y), the power spectral density PSD is equal to the square of the Fourier transformation F(u, v) of the surface function I(x, y). The power spectral density function is defined as;

$$S(u,v) = \left|F(u,v)\right|^2 \quad (7)$$

Where u and v are the spatial frequencies (number of waves per unit wave length) in the x and y directions respectively. The PSD is converted to the polar coordinate system S (f), such that $f = \sqrt{u^2 + v^2}$. The value of S(f), at each radial frequency f, is averaged over angular distributions. The slope of the linear regression line β is related to FD by equation [18]:

$$FD = \frac{8-\beta}{2} \quad (8)$$

It is reported in the related literature that fractal dimension and intercept are significant fractal parameters that describe the irregularity and complexity of the surfaces. Moreover, the intercept correlates well with the overall magnitude of roughness of the observed texture appearance of the surface images. In the present study, fractal analysis is going to be used to assign numerical values to indicate the development of pitting corrosion.

3. EXPERIMENTAL PROCEDURE

Carbon steel is the most widely used engineering material, so the cost of dealing with corrosion of carbon steels is a significant portion of the total cost of corrosion. Carbon steel test coupons with dimensions of 50×30×1 mm were cut from a single sheet to ensure metallurgical uniformity. The surface roughness is known to play an important role in developing the corrosion [28,29], Therefore the coupon's working faces were polished with grade 800 silicon carbide paper. A typical

polished surface is shown in Fig.1. The inclined vertical lines shown in the photo are the traces of polishing

A rotating corrosion-test equipment was used for studying pitting corrosion behavior. The coupons were immersed in 1200 ml open pot having 700 ml of tap water. The pot was fitted with four vertical baffles to break up the rotational flow pattern. The pot and the baffles were made from plastic material. Each coupon was attached to a rotating shaft with pvc washers and a plastic screw to avoid the galvanic corrosion. Because of the rotational speed, turbulence was generated in the test water, together with a tendency for a rise in test water temperature. Since the test water temperature markedly affects the corrosion rate [27], the test water was changed every one hour. The temperatures at the beginning and the end of test were 23 oC and 24 oC, respectively. Table 1 shows the composition of test water determined by chemical analysis.

Coupons were rotated at 160 rpm (linear velocity of 0.5 m/s) for test periods of 1, 3, 5, and 7 h. At the end of test period the rotating shaft with coupon was withdrawn, and air dried. The corroded surfaces were examined by a Scanning electron microscope (SEM). These digitized SEM images were used in the image analysis to develop features to characterize the pits development with the time.

Table 1 Chemical analysis of test water

Elements	Na^+	Ca^{2+}	Mg^{2+}	K^+	HCO_3^-	Cl^-	Fl^-	NO_3^-	SO_4^{-2}	pH	TDS
	37.8	75.2	6.8	2.7	70.2	73.3	0.28	2.6	10.7	7.2	350

Note: all values except pH are in mg/l

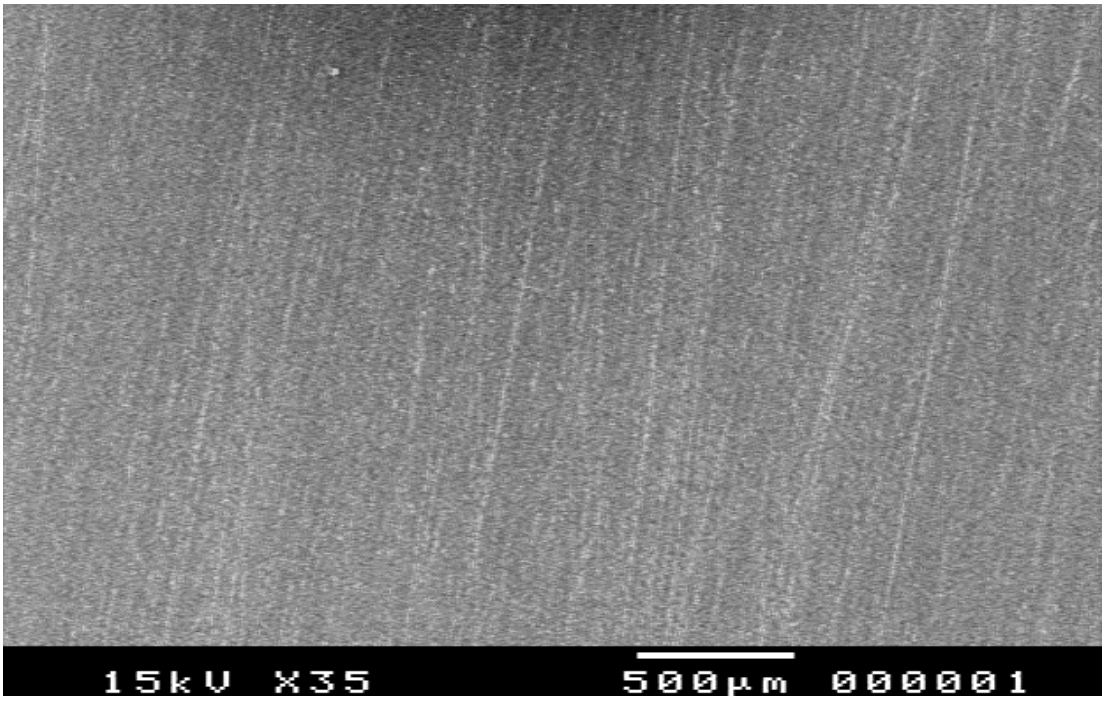

Fig.1: Showing the polished surface before test

4. RESULTS AND DISCUSSION

4.1 Morphology of Pitting Corrosion

The typical corrosion pits formed on the polished surfaces rotated in tap water at different times are shown in Fig. 2. It can be observed that many pits are formed on the surface and each pit formed has a track accompanied it which appears as black in photos and which looks like a comet streak tail. The characteristic features of these pits are the presence of two parts: a cavity at the pit centre and a rough circular band around the cavity, which is labeled 1, as well as circular rings, labeled 2. The same shape for these pits has been observed

before in the literature on corrosion tests [19-23]. The comet tails were formed in opposite direction to the rotation of the specimen. The comet tails take the form of cone tubular structure. The circular base of cone is the ring that formed around the inclusion. The effect of time on the pitting corrosion development for rotation test is illustrated from the photo, where the pit and the comet size increase with the time. It can be seen in these photos that many pits formed and material removed along the track direction. This gives evidence that the corrosion products are aggressive. This is in agreement with that reported in Ref. [23].

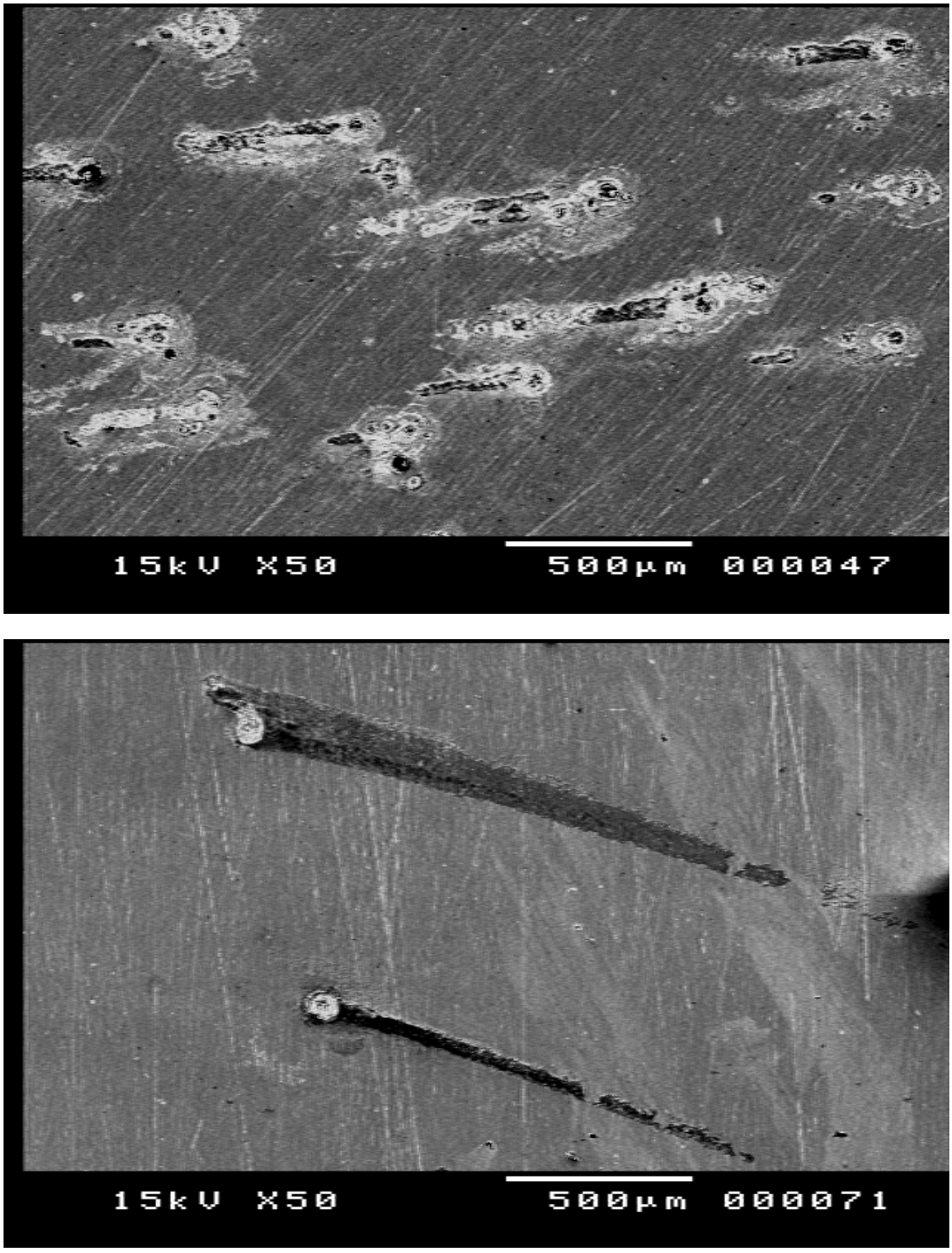

Fig 2 Continue

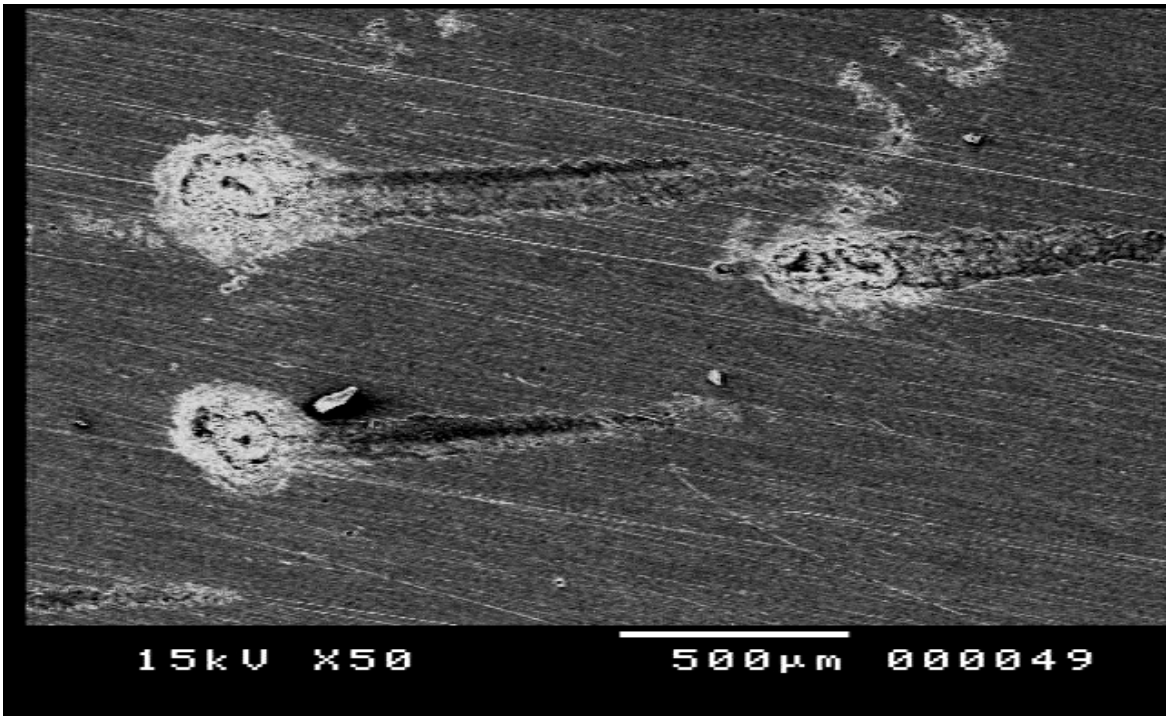

Fig 2 Continue

4.2 Feature Extraction of Pits Development

In the present section, the features parameters of images such as wavelet entropy, wavelet energy, and fractal dimension and intercept value are extracted. The results of these feature parameters, performed by using 2D-DWPT and fractal analysis and described in Ch.2 are given in Figs 3-6. Shannon entropies and energy of wavelet packet decomposition of image were calculated with the testing time from all the selected subbands of the image as shown in Figs. 3 and 4. Figures 5 and 6 show the fractal dimensions and intercept for the image of corroded surface at different times. From these figures, it is clear that the value of the entropy, energy, fractal dimension and intercept increases with time. Each feature corresponds to a visually recognizable property of the image described in Sec. 4.1. That is, for undamaged surfaces which have homogeneous textures have relatively low values of entropy, energy, fractal dimension and intercept. While, these extracted features have high values for corroded surfaces due to the coarseness of the corroded surface textures.

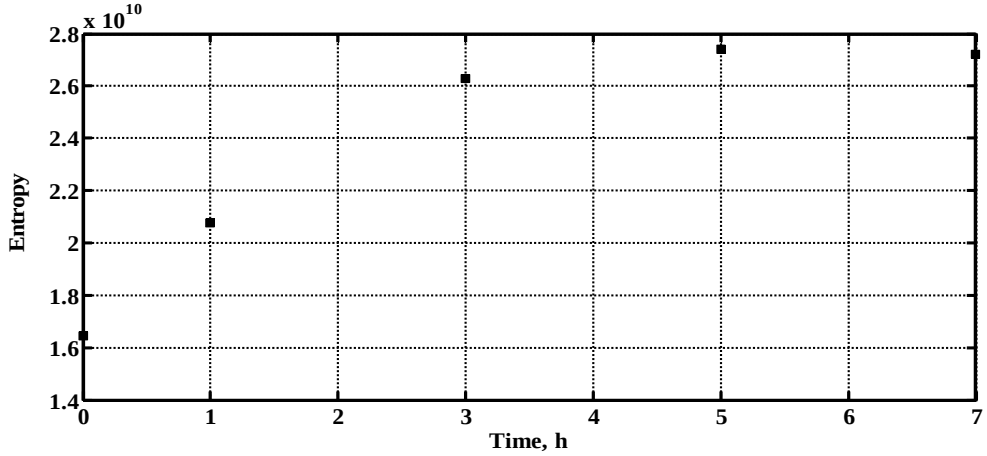

Fig. 3 Change of Shannon entropy with test time

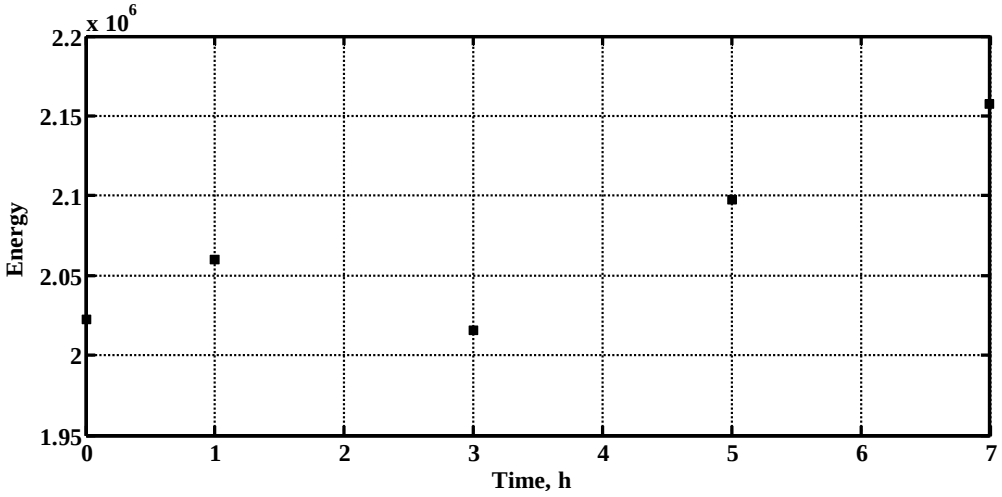

Fig. 4 Change of energy with test time

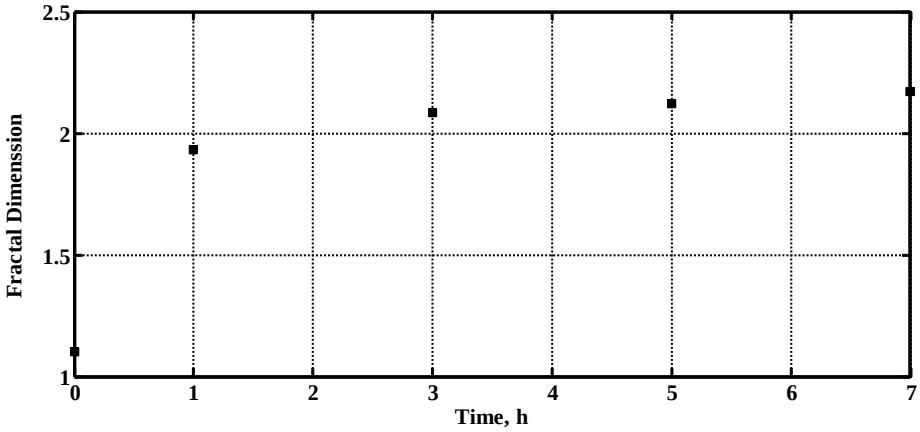

Fig. 5 change of fractal dimension with test time

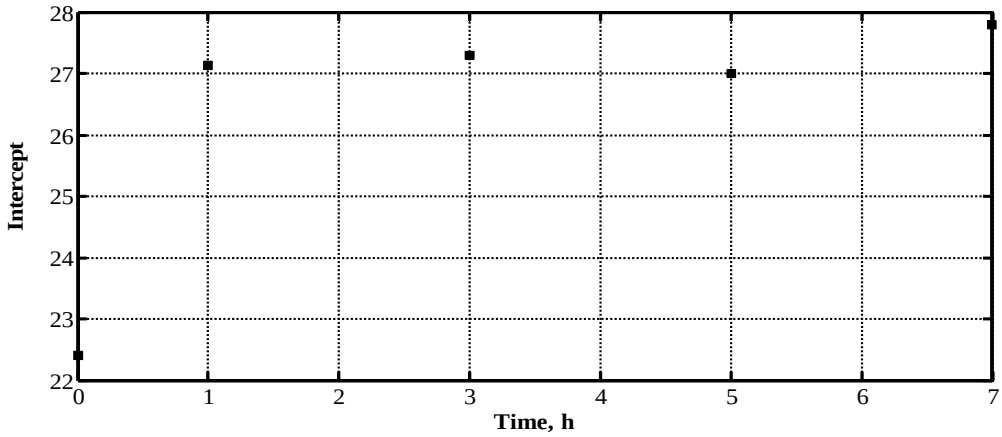

Fig. 6 change of fractal intercept with test time

CONCLUSIONS

Image processing based on discrete wavelet transform and fractal analysis was used to characterize the corroded damage images. The following results can be drawn:

(1) The extracted feature parameters; Shannon entropy, energy loss, fractal dimension and fractal intercept increase with exposure time..

(2) The results indicate that the image analysis procedures are promising techniques since they are effective in characterizing the changes of surface topography with exposure time.

(3) The surface topography with test time showed that a tubular corrosion product structure developed with corrosion pit in reverse direction of rotation.

REFERENCES

[1] Frankel, G. S.: Pitting Corrosion of Metals A Review of the Critical Factors. J. Electroch. Soc. 145(6), pp. 2186-2198, (1998)

[2] Davis, R.J.: Corrosion: Understanding the Basics. ASM International, (2000)

[3] Bardal, E.: Corrosion and Protection. Springler verlag, (2004)

[4] Jones, D. : Principles and Prevention of Corrosion", Prentice-Hall, (1996)

[5] MAlik,A.U., Al Fawzan, S.: Localized corrosion Of AISI 316L SS in Arabian Gulf seawater, Desalination, 123, pp. 205-213, (1999)

[6] Li,G.B., Li, T.J.: Extracting characteristics from corrosion surface of carbon steel based on WPT and SVD,Z. Qian et al. (Eds.): Recent Advances in CSIE 2011, LNEE, Springer-Verlag Berlin Heidelberg, pp. 105-112, (2012)

[7] Gao,Z.M, Han, X. B., Dang, L.H., Wang, Y., Bi, H.C.: Evaluation of simulated atmospheric corrosion of Q235 steel by wavelet packet image analysis, Int. J. Electrochem. Sci., 7, pp. 9202-9212, (2012)

[8] Tao,L. , Song,S.Z., Zhang,X.Y. , Zhang, Z., Lu ,F.:Image analysis of atmospheric corrosion of field exposure high strength aluminum alloys, Appl. Surf. Sci., 254, pp. 6870-6874,(2008)

[9] Wang, S., Song,S.: Image analysis of atmospheric corrosion exposure of zinc, Mater. Sci. Eng. A 385, pp. 377–381, (2004)

[10] Pereira, M. C., Silva,J.W. J. , Acciari,H.A., Codaro,E. N. , Hein L.R. O. : Morphology Characterization and Kinetics Evaluation of Pitting Corrosion of Commercially Pure Aluminium by Digital Image Analysis, Materials Sciences and Applications, 3,pp. 287-293, (2012

[11] Pidaparti, R.M., Aghazadeh, B.S., Whitfield ,A., Rao, A.S., Mercier, G.P. : Classification of corrosion defects in NiAl bronze through image analysis. Corrosion Science, 52, pp.3661–3666, (2010).

[12] Chenghao, Li., Wei, ZA. : Fractal characteristic of pit distribution on 304 stainless steel corroded surface and its application in corrosion diagnosis, J. Wuhan Univ. Techn-mater, Sci. Ed., pp.389-393, 920070

[13] Codaro, E.N., Nakazato, R.Z., Horovistiz, A.L., Ribeiro L.M.F., Ribeiro,R.B., Hein, L.R.O.: An image processing method for morphology characterization and pitting corrosion evaluation, Mater. Sci. Eng. A 334, pp. 298-306, (2002)

[14] Huang, K., Aviyente, S.: Wavelet Feature Selection for Image Classification IEEE Trans. Image Process., 17(9), pp. 1709-1720, (2008)

[15] Mallat, S.:A wavelet tour of signal processing, Academic, New York, (1999)

[16] Russ, J. C. :Fractal analysis, Encyclopedia of Material: Science of Technology, Elsevier Science Ltd., 3247–3254(2001)

[17] Zhang, J.: Detection and monitoring of wear using imaging methods, Ph.D. thesis, University of Twente, Enschede, The Netherlands, (2006)

[18] Babadagli, T., Develi, K.: Fractal analysis of natural and synthetic fracture surfaces of geothermal reservoir rocks, Proc. World Geothermal Congress 2000 Kyushu - Tohoku, Japan, May 28 - June 10 (2000)

[19] Budiansky, N.D., Hudson, J.L., Scully, J.R.: Origins of persistent interactions among localized corrosion sites, Symp. in Honor of Hans Bohni, Electrochemical Society, Salt Lake City, UT, (2002)

[20] Wang, W., Zhang, X., Wang, J.: Pits with colored halos formed on 1Cr18Ni9Ti stainless steel surface after ennoblement in seawater. Mater. Sci. Eng. C 29, pp. 851–855, (2009)

[21] Karrab,S.A., Doheim, M. A., Mohamed S. Mohammed, Ahmed,S.M.: Study of cavitation erosion pits on 1045 carbon steel surface in corrosive waters. ASME, J. Tribol 134, 0011602- pp. 1-6, (2012)

[22] Karrab,S.A., Doheim, M. A., Mohamed S. Mohammed, Ahmed,S.M.: Investigation of the ring area formed around cavitation erosion pits on the surface of carbon steel. Tribol Lett 45, pp. 437-444, (2012)

[23] Alkanhal Tawfeeq A. , Osman M., Ahmed, S. M.: investigation into tubular structure formed by pitting corrosion on the surface of carbon steel, J. Eng. Sci., (Assiut Univ, Egypt) 33 (6), 2165 (2005)